EPR and charge transfer in H_2SO_4-doped polyaniline

V. I. Krinichnyi
Institute of Problems of Chemical Physics of Russian Academy of Sciences, Chernogolovka, 142432 M.R., Russia

H. -K. Roth
Thüringean Institute for Textil and Polymer Research, Dept. of Physical Research, Breitscheidstr. 97, D-07407 Rudolstadt, Germany

G. Hinrichsen
Institute of Nonmetallic Materials, Department of Polymer Physics, Technical University of Berlin, Englische Str. 20, D-10587 Berlin, Germany

F. Lux
Patent Management and Corrosion Control Consulting, Calvinstrasse 14, D-10557 Berlin, Germany

K. Lüders
College for Technology, Economy and Culture, Dept. Informatic, Mathematics and Natural Sciences, PF 66, D-04251 Leipzig, Germany
(Received 16 October 2001; published 27 March 2002)

The study of the electron relaxation and dynamics of polaron charge carriers in undoped and H_2SO_4-doped polyaniline (PANI) by means 3-cm (9.7 GHz) and 2-mm (150 GHz) EPR spectroscopy, and ac, superconducting quantum interference device, and dc conductometries is reported. The existence in PANI of polarons with different relaxation and mobility is shown. Spin-lattice and spin-spin relaxation times as well as the intrachain diffusion and interchain hopping rates of these centers were determined separately at 90–330 K by a steady-state saturation method at 2-mm waveband EPR. At the polymer doping an effective spin relaxation decreases due to the formation of metal-like domains of well-coupled chains with three-dimensional (3D) delocalized charge carriers. The mechanism of spin and charge transfer in PANI with different doping levels is analyzed. The macroconductivity and microconductivity of the medium-doped PANI is determined by 3D interdomain and intradomain hopping of charge carriers, respectively. In a heavily doped polymer 1D interdomain and 3D interchain Mott variable range charge hoppings dominate, accompanied with a strong interaction of the charge with the lattice phonons. It is shown that a bipolaron is the preferred charge carrier in doped PANI samples.

DOI: 10.1103/PhysRevB.65.155205 PACS number(s): 72.80.Le, 75.50.Pp, 76.30.Rn, 71.38.Fp

I. INTRODUCTION

Among conducting polymers,[1] polyaniline (PANI) and its derivatives in recent years have been at the center of considerable scientific interest due to their relatively high conductivity, environmental stability, and ease of preparation in raw materials.[2] In PANI a nitrogen heteroatom is incorporated between phenyl rings in the backbone of the chain, which results in the essential difference in its properties. PANI generally exists in two main forms, an emeraldine base (PANI-EB) and an emeraldine salt (PANI-ES) (Fig. 1).[2]

The fully reduced PANI-EB is an insulator with a conductivity $\sigma \sim 10^{-10}$ S/cm. The ''metallic'' PANI-ES, with a conductivity of $\sigma \sim 4 \times 10^{2}$ S/cm is obtained upon protonation of the EB by exposure to protonic acids or upon oxidative doping of the EB.[2] The fundamental interest in polyaniline stems from the possibility of investigating physics in different states, such as the ''Fermi glass'' state,[3] the ''granular metal'' state,[4] or as a ''disordered metal'' close to the metal-insulator transition state.[5] The fundamental properties of PANI depend on the mechanisms of charge transfer in this polymer. The presence of localized electronic states of energies less than the band gap arising from changes in local bond order, including the formation of polarons and bipolarons, has led to the possibility of different types of charge conduction in PANI and other poly(*p*-phenylene)-like polymers.[6]

Variations in the electrical, magnetic, and optical properties of the emeraldine forms of PANI differ from the results of studies of poly(*p*-phenylene)-like polymers.[7] Polyaniline is not charge conjugation symmetric, that is, the Fermi level and band gap are not formed in the center of the band, so that valence and conduction bands are quite asymmetric, with only a half-occupied polaron band deep in the gap as opposed to the typical two bands in a normal conducting polymer.[8] In addition, the electronic state of the polymer can

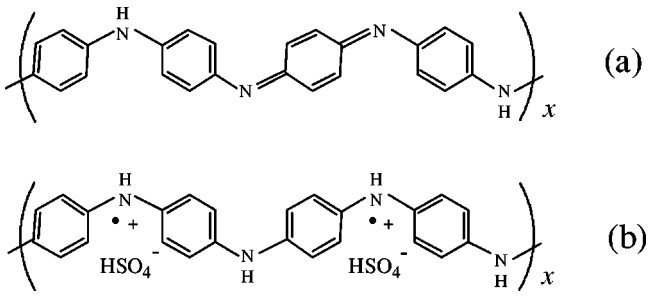

FIG. 1. Schematic structure of (a) the emeraldine base form of polyaniline (PANI-EB), and (b) the heavily doped emeraldine salt form of polyaniline in the polaron lattice state (PAN-ES).

be changed through a variation of either the number of electrons per repeat unit through electrochemical doping (while holding the number of protons constant) or the addition (or subtraction) of protons associated with individual nitrogen sites (while holding the number of electrons on the polymer constant).

There has been increasing interest in the temperature and composition behavior of the conductivity of PANI and in the mechanism of this conduction. Frequency-dependent conductivity measurements of partly protonated emeraldine were proposed to support the presence of an interpolaron hopping mechanism.[9] The effects of protonation on the emeraldine base led to a proposal of the transformation of its electronic structure to that of a granular polaron metal.[10] For intermediate protonation levels, magnetic and optical experiments supported the phase segregation between highly conducting regions and the insulating background.[11] It was proposed that the charge conduction is via charging energy-limited tunneling among the small granular polymeric grains.[12]

A detailed study by different methods of PANI-ES (Refs. 10, 13, and 14) allowed one to conclude that both chaotic and oriented PANI-ES's consist of some parallel chains strongly coupled into ''metallic bundles'' between which one-dimensional (1D) variable range hopping (VRH) charge transfer occurs and in which electrons are three-dimensionally delocalized. The intrinsic conductivity of these domains was evaluated using a Drude model as $\sigma \sim 10^7$ S/cm,[15] which was very close to value expected by Kivelson and Heeger for the metal-like domains in heavily doped Naarmann *trans*-polyacetylene (*trans*-PA).[16] However, the ac conductivity of the sample does not exceed ~ 700 S/cm at 6.5 GHz.[15] PANI-HCl is characterized by the density of the states $n(\varepsilon_F) \cong 3.5$–$3.8$ states/eV per two rings at the Fermi level ε_F.[17,18]

From the optical reflectance study of PANI doped by different counterions, Lee *et al.*[19] showed that, in contrast to other PANI-ES's, PANI-H_2SO_4 should be considered as a Fermi glass in which the electronic states $n(\varepsilon_F)$ are localized due to disorder. From an analysis of the band structure it was concluded that PANI-H_2SO_4 can be considered more metallic than PANI-HCl .

The macroscopic conductivity of the polymers often may reflect a superposition of several charge transport processes. Therefore, intrinsic charge transfer along a chain is the most difficult property to examine by the usual experimental methods, as it can be masked by interchain, interglobular, and other processes. Inhomogeneities in structure and doping can also contribute to this complexity. As nonlinear excitations possess an unpaired electron with spin $S=1/2$, the magnetic resonance methods EPR and NMR allow one to study spin carrier motions on the scale of even few polymer units. One of the advantages of the methods is the possibility to determine the coefficient of spin diffusion along (D_{1D}) and between (D_{3D}) polymer chains, and thus the anisotropy $A = D_{1D}/D_{3D}$ of such a motion, even for polymer with chaotically oriented chains.

Spin and charge dynamics was studied mainly in PANI-HCl.[20,21] Mizoguchi *et al.*[21] found from both proton and electron relaxation data that the D_{1D} value is 10^{12}–10^{14} rad/sec, and depends weakly on the polymer doping. The D_{3D} value of PANI-ES was shown to be $D_{3D} \cong 6 \times 10^{11}$ rad/s, so then $D_{1D}/D_{3D} \sim 10^3$ at room temperature, and it depends on the doping level and correlates with corresponding dc and intrinsic conductivities. This fact was attributed to the existence of conducting domains as solitary single polymer chains even in heavily doped PANI. This supposition corresponds to the data,[22] but contradicts the concept of metal-like islands diluted in an amorphous phase of the polymer.[10,13] Therefore, it was still not clear in interpretations of different experimental data concerning electronic processes in this PANI. Recently, Krinichnyi *et al.*[18] investigated PANI-HCl in detail by high-field EPR, and dc and microwave conductivity techniques. They showed that quasi-3D charge hopping between pinned and mobile small polarons dominates the bulk conductivity of PANI-EB. The conductivity of slightly doped PANI-HCl is determined by the isoenergetic charge hopping between the polaron and bipolaron states, whereas charge transfer in heavily doped PANI-HCl can be described as a superposition of 1D VRH and charge scattering on the phonons of metal-like islands (with 3D delocalized charge carriers).

Up to now the spin relaxation and dynamics parameters of PANI-H_2SO_4, as well as the charge transfer process in the polymer, have not been studied. Here we report detailed results of multifrequency (9.7–150 GHz) EPR, dc and microwave (150 GHz) conductivity and ac susceptibility studies of H_2SO_4-doped polyaniline. We study the spin relaxation and mobility of polaron charge carriers. As in the case of PANI-HCl, we show the existence in PANI-H_2SO_4 of polarons with different relaxation and mobility. The charge in undoped PANI hops isoenergetically between polaron-bipolaron pairs. Upon the doping of the polymer the charge carriers start to scatter on the lattice phonons in 3D metal-like domains. In heavily doped PANI the charge carriers were shown to be transferred in the framework of the variable range hopping mechanism and the undimerized Su-Schrieffer-Heeger model. Some results on undoped and H_2SO_4-doped PANI were briefly reported previously.[23]

II. EXPERIMENTAL METHODS AND RESULTS

A. Preparation of the samples

Conductive PANI powder samples were first obtained by polymerization via a modification of the general oxidation route with $(NH_4)_2S_2O_8$ in 1.0-M hypochloric acid.[24] To obtain samples of different doping levels *y*, individual amounts of 2 g of the undoped powder were equilibrated by stock solutions with $p\mathrm{H}=0$–14. The doping level $y=[S]/[N]$ was determined on the basis of an elemental analysis.

B. Direct current conductivity

The dc conductivity of the pelletlike low- or high-conductive samples was measured in the 6–300-K temperature region in an inert atmosphere using the two- or four-probe methods, respectively. Figure 2 shows the change in dc

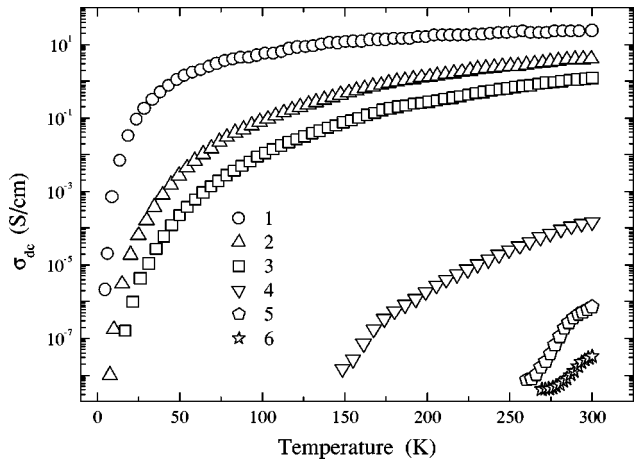

FIG. 2. Temperature dependences of the dc conductivity of PANI samples with doping levels $y=0.53$ (1), 0.42 (2), 0.21 (3), 0.06 (4), 0.03 (5), and 0.01 (6).

conductivity of H_2SO_4-doped emeraldine polyaniline samples as a function of temperature.

C. Electron paramagnetic resonance

EPR experiments were performed using a 2-mm waveband ($\nu_e=150$ GHz, *D* band) EPR-05 (Ref. 25) and a 3-cm waveband ($\nu_e=9.7$ GHz, *X* band) PS-100*X* spectrometers with 100-kHz field ac modulation for phase-lock detection. The total spin concentration in the samples was determined using a $Cu_2S0_4\cdot 5H_2O$ single crystal standard, whereas Mn^{2+} with $g_{eff}=2.00102$ and $a=87.4$ G was used for the determination of *g* factor as well as for the magnetic field sweep scale calibration at the 2-mm waveband. 3-cm waveband EPR signals of the samples, placed into quartz ampoules with an inert atmosphere, were registered in the 90–300-K temperature range. At the 2-mm waveband EPR their spectra were recorded for imaginary, $\chi^{|}$, and real, $\chi^{\|}$, terms of the total paramagnetic susceptibility in the 90–330-K temperature range in an inert atmosphere. The error in the determination of the peak-to-peak linewidth ΔB_{pp} and the *g*-factor values was $\pm 2\times 10^{-2}$ G and $\pm 2\times 10^{-4}$ at the 3-cm waveband, and $\pm 5\times 10^{-2}$ G and $\pm 2\times 10^{-5}$ at 2-mm waveband EPR, respectively. The spectra were simulated using MICROCAL ORIGIN V6.0 and WINEPR SIMFONIA V1.25 (Bruker) programs.

Figure 3 shows 3-cm and 2-mm waveband EPR spectra of an initial, emeraldine base PANI sample, and emeraldine salt PANI samples doped with different numbers of sulfuric acid molecules. Undoped PANI at the 3-cm waveband demonstrates a Lorentzian three-component EPR signal consisting of asymmetric (R_1) and symmetric (R_2) spectra of paramagnetic centers (PCs) which can be attributed to localized and delocalized unpaired electrons [Fig. 3(a)], respectively. R_2 PC's keep line symmetry at $y\leqslant 0.42$ doping levels. At the 2-mm waveband the PANI EPR spectra became Gaussian and broader compared with 3-cm waveband ones [Fig. 3(b)], as is typical of PCs in other conducting polymers.[26] At this waveband R_2PCs demonstrate an asymmetric EPR spectrum at all doping levels.

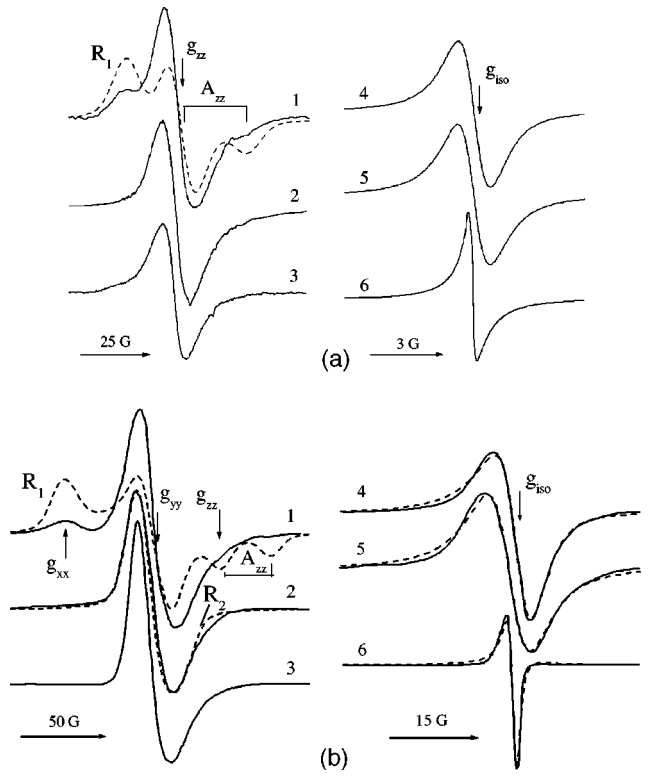

FIG. 3. Absorption spectra of PANI samples with doping levels $y=0.00$ (1), 0.01 (2), 0.03 (3), 0.21 (4), 0.42 (5), and 0.53 (6), registered at room temperature at (a) 3-cm and (b) 2-mm waveband EPR. The spectra of radical R_1 calculated with $g_{xx}=2.006032$, $g_{yy}=2.003815$, $g_{zz}=2.002390$, $A_{xx}=A_{yy}=4.5$ G, $A_{zz}=30.2$ G, and radical R_2 calculated with $g_{\perp}=2.00439_4$ and $g_{||}=2.00376_3$ are shown at left. By the dashed lines the spectra (b) calculated from Eq. (2) with $D/A=1.9$ (above), 6.3 (middle), and 1.2 (below) are shown as well.

At the 2-mm waveband in both in-phase and out-of-phase $\pi/2$ components of the dispersion EPR signal of neutral and slightly doped PANI, the bell-like contribution with Gaussian spin packet distributions is registered (Fig. 4). This effect was not observed earlier in studies of conducting polymers at lower registration frequencies.[27] The appearance of such a component is attributed to the adiabatically fast passage of the saturated spin packets by a modulating magnetic field, as discussed below.

The plots of the 3-cm, 2-mm waveband peak-to-peak linewidth ΔB_{pp} vs temperature and doping level for PC in PANI samples are shown in Fig. 5. It is seen from the Fig. 5 that ΔB_{pp} of R_2 PC's depends on both the doping level and temperature. At the 3-cm waveband EPR the linewidth of PC's in PANI with $y\leqslant 0.21$ depends weakly on the temperature, whereas this value of PANI samples with $y\geqslant 0.42$ demonstrates a greater sensitivity to temperature. At this waveband the value of ΔB_{pp} increases with the temperature decrease down to some critical temperature $T_c\cong 200$ K. At lower temperatures the linewidth of PANI with $y=0.21$ continues to increase, however, this value of heavily doped PANI samples starts to decrease at T_c (Fig. 5). At the 2-mm waveband the T_c value shifts down to 140 K. The sensitivity of

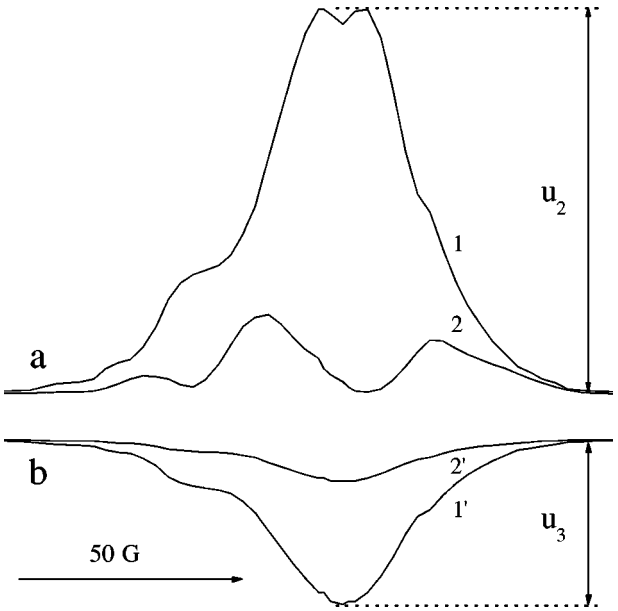

FIG. 4. The typical in-phase (a) and out-of-phase (b) $\pi/2$ of the dispersion spectrum components of PANI samples with $y \leqslant 0.1$ registered at $B_1 \geqslant B_{1_0}(1,1')$ and $B_1 \approx B_{1_0}(2,2')$ at room temperature.

the linewidth of PANI with $y=0.53$ to temperature disappeared at higher registration field [see Fig. 5(b)].

The temperature dependence of the total paramagnetic susceptibility of PC's in some PANI samples was determined using double integration of their EPR spectra (Fig. 6). Spin-lattice and spin-spin relaxation times of undoped and slightly doped PANI samples were measured separately at 2-mm waveband EPR using the cw saturation method described in detail earlier.[28]

D. Magnetic susceptibility

The measurements of magnetic susceptibility of the PANI samples were performed at room temperature by the superconducting quantum interference device (SQUID) method, as described in Ref. 24. The data obtained are presented in Table I.

III. DISCUSSION

A. Direct current conductivity

The dc conductivity of the samples shown in Fig. 2 can be described in the framework of the Mott VRH of charge carriers between crystalline high-conducting regions through amorphous bridges.[29] The mechanism is based upon the idea that carriers tend to hop larger distances to sites which lie energetically closer rather to their nearest neighbors. According to this model, the dc conductivity is given by the temperature function

$$\sigma_{dc}(T)=e^2\nu_0\sqrt{\frac{9n[n(\varepsilon_F)]}{8\alpha k_B T}}\exp[-(T_0^{|}/T)^{-1/(1+d)}]$$
$$=\sigma_0 T^{-1/2}\exp[-(T_0^{|}/T)^{-1/(1+d)}], \quad (1)$$

where e is the elemental charge, ν_0 is a hopping frequency, $n(\varepsilon_F)$ is the density of states at the Fermi level ε_F determined from Pauli susceptibility as $\chi_P=\mu_B^2 n(\varepsilon_F)$, μ_B is the Bohr magneton, α^{-1} is the decay length of the localized electron state, k_B is the Boltzmann constant, T is the temperature, d is a dimensionality of the system, and $T_0^{|}$ is the percolation constant or the characteristic temperature, above which the conductivity is essentially determined by the phonon bath, and below which it is determined by the distributional disorder of electron states in space and energy. The intrinsic percolation constant T_0 is determined from the relations[30] $T_0'=2T_0$ at $d=1$ and $T_0'=512T_0\ln^2(4T_0/\pi t_{\perp})$ at $d=3$, where $t_{\perp}$ is the transfer integral, which denotes interchain exchange between nearest-neighbor chains. The T_0 value is equal to $16\alpha/k_B z n(\varepsilon_F)$ at $d=1$ (here z is the num-

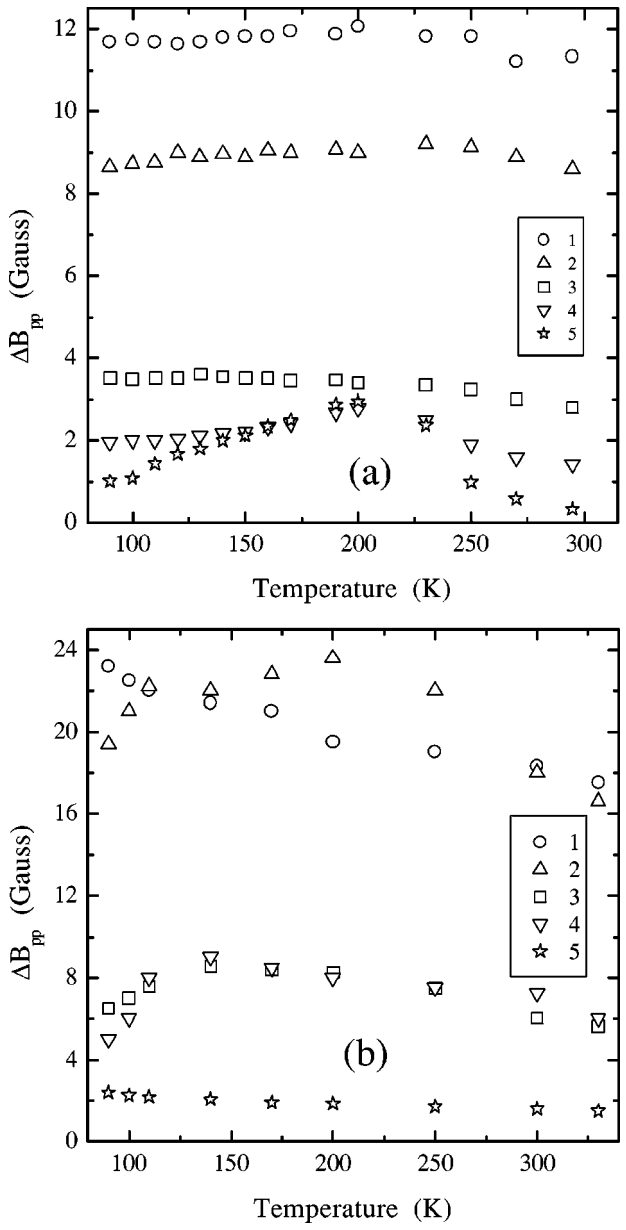

FIG. 5. Temperature dependence of the peak-to-peak linewidth, ΔB_{pp} of (a) 3-cm and (b) 2-mm waveband absorption EPR spectra of PC R_2 in PANI samples with doping levels $y=0.00$ (1), 0.03 (2), 0.21 (3), 0.42 (4), and 0.53 (5) adjusted for the Dyson contribution.

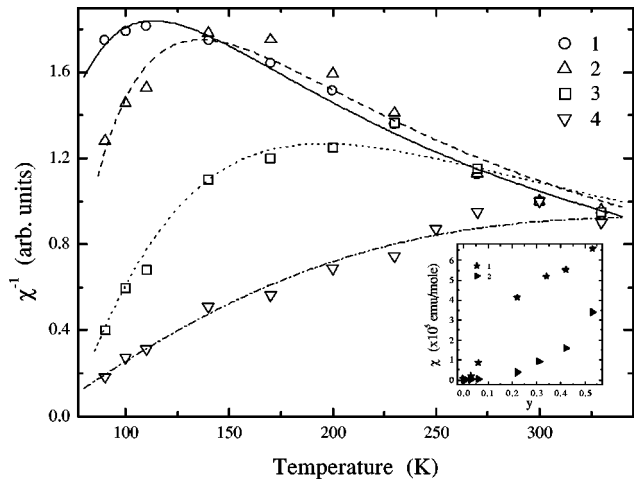

FIG. 6. Temperature dependence of the inverted paramagnetic susceptibility of PC in PANI samples with doping levels $y=0.53$ (1), 0.21 (2), 0.03 (3), and 0.00 (4). Inset: Pauli susceptibility (1) determined by SQUID and paramagnetic susceptibility (2) obtained from 2-mm waveband EPR spectra of PANI with different doping levels y. Also shown are the dependences calculated from Eq. (3) with $N_C/N_{TA}=1.3/1$, $\theta=42.8$ K, and $J=0.144$ eV (solid line), $N_C/N_{TA}=1/1$, $\theta=65.5$ K, and $J=0.108$ eV (dashed line), $N_C/N_{TA}=2.8/1$, $\theta=72.7$ K, and $J=0.120$ eV (dotted line), and $N_C/N_{TA}=16.5/1$, $\theta=59.6$ K, and $J=0.130$ eV (dash-dotted line).

ber of nearest-neighbor chains, which is four for polyaniline[10]) and to $18\alpha^3/k_B n(\varepsilon_F)$ at $d=3$.[31] The distance R and average energy W of the charge carriers hopping can be estimated, respectively, as $R^{-4}=(8/9)\pi\alpha k_B T n(\varepsilon_F)$ and $W^{-1}=(4/3)\pi R^3 n(\varepsilon_F)$.

By plotting $\sigma_{dc}T^{1/2}$ as a function of $T^{-1/2}$ or $T^{-1/4}$ a straight line for the samples under study should be obtained, in agreement with Eq. (1). It is seen from Fig. 7 that Eq. (1) with $d=1$ and 3 fits well the value $\sigma_{dc}(T)$ obtained for PANI-H_2SO_4 with $y=0.53$ and $y\leqslant 0.42$, respectively. The values of parameters T_0 and α^{-1}, obtained from the slope and from the intersection with the conductivity axis, respectively, are presented in Table I. The calculated $n(\varepsilon_F)$, R, and W values are summarized in Table I as well.

A transition from localization to delocalization occurs when K is equal to a unit where $K=(\pi^2/2^{1/2})(t_\perp/4T_0)$ and $t_\perp=(2e^2/\varepsilon a)(r/a)\exp(-r/a)$, and ε is the background dielectric constant of the polymer mainchain.[13] Using $r=0.35$ nm, $a=0.106$ nm, and $\varepsilon=4$, then $t_\perp=0.29$ eV, and T_0 is experimentally determined; thus we obtain the K value for the PANI samples (see Table I). An increase in the K value with y means increasing the charge-carrier delocalization as a result of an increase in the interchain coherence. This value is higher than unity for heavily doped PANI-HCl,[30] and decreases down to 0.1–0.4 for heavily doped derivatives of polyaniline, namely, poly(*o*-toluidine) and poly(*o*-ethylaniline).[32]

It may be noted that $\alpha R\leqslant 1$ for PANI-H_2SO_4, with $y\geqslant 0.21$ and $W\cong 0.01$ eV ($y=0.53$), are quite consistent with Mott's requirements that αR should be comparable to the unit and W to k_BT in order to hop to distant sites. One can conclude that the insulator-to-metal transition in PANI-H_2SO_4 is of localization-to-delocalization type, driven by the increased structural order between the chains and through an increased interchain coherence. PANI-H_2SO_4, with $y=0.53$, possesses a more metallic behavior, and the properties of PANI-H_2SO_4 with $y\leqslant 0.42$ demonstrate it to be near an insulator/metal boundary. The inherent disorder present in slightly doped PANI keeps the electron states localized on individual chains. At low y the structural disorder in polyaniline localizes the charge to single chains (Curie-like carriers), and the higher doping leads to the appearance of delocalized electron states (Pauli-like carriers). This holds typically for the formation in PANI with $y\geqslant 0.21$ metal-like domains, according to the island model proposed by Wang and co-workers.[10,13] This conclusion would be consistent

TABLE I. Pauli (χ_P) and paramagnetic (χ_s) susceptibility, determined respectively by the SQUID and EPR methods, the density of states $n(\varepsilon_F)$ at the Fermi level ε_F, the percolation constant T_0, the decay length of the localized electron state α^{-1}, the charge carriers hopping distance R and the average hopping energy W, the charge localization factor K, and the constants of an antiferromagnetic spin interaction θ and J, determined for PANI samples with different doping level y.

Value	Doping level y						
	0.00	0.01	0.03	0.06	0.21	0.42	0.53
χ_P, $\times 10^6$, emu/mole	0.5	0.55	0.6	0.64	51	86	101
χ_s, $\times 10^6$, emu/mole	0.18	0.21	0.43	0.62	3.83	16.0	34.1
ε_F, states/eV two rings	~0	0.01	0.02	0.19	1.3	1.8	2.8
ε_F, eV	-	-	-	-	0.10	0.33	0.51
T_0, $\times 10^{-3}$ K	-	-	-	96.5	7.87	5.65	1.73
α^{-1}, nm	-	-	-	0.97	1.7	1.9	2.9
R, nm	-	-	-	2.12	1.55	1.54	1.58
W, eV	-	-	-	0.042	0.018	0.016	0.011
K	-	-	-	2.1	0.91	0.81	0.54
θ, K	59.6	-	72.7	-	65.5	-	42.8
J, eV	0.130	-	0.120	-	0.108	-	0.144

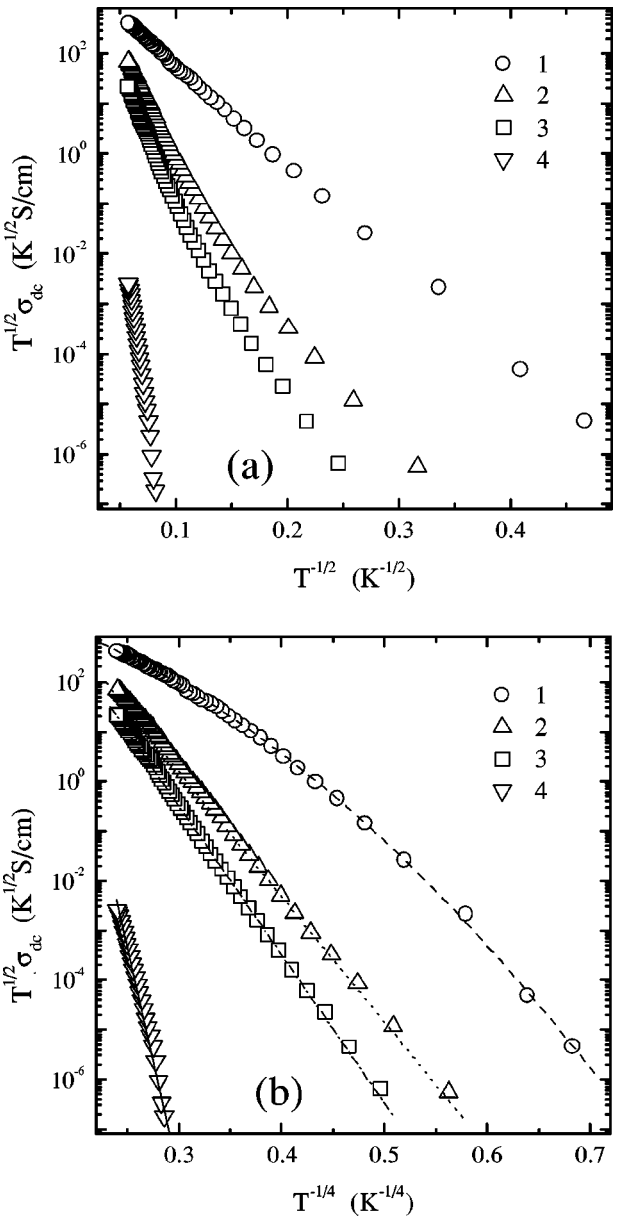

FIG. 7. Plots of the $\sigma_{dc}T^{1/2}$ multiplicity as a function of $T^{-1/2}$ (a) and $T^{-1/4}$ (b) obtained for PANI samples with doping levels $y=0.53$ (1), 0.42 (2), 0.21 (3), and 0.06 (4). The lines show the dependences calculated from Eq. (1) with $\sigma_{dc}^{0}=1.17\times10^{5}$ S $K^{-1/2}$ cm^{-1} and $T_0'=3.46\times10^{3}$ K (dashed line), $\sigma_{dc}^{0}=5.12\times10^{9}$ S $K^{-1/2}$ cm^{-1} and $T_0'=1.65\times10^{7}$ K (dotted line), $\sigma_{dc}^{0}=2.02\times10^{10}$ S $K^{-1/2}$ cm^{-1} and $T_0'=2.97\times10^{7}$ K (dash-dotted line), and $\sigma_{dc}^{0}=5.22\times10^{18}$ S $K^{-1/2}$ cm^{-1} and $T_0'=1.35\times10^{9}$ K (solid line) in appropriated coordinates.

with that drawn earlier on the basis of data obtained with TEM and X-ray-diffraction methods.[23]

B. Magnetic resonance parameters

As seen from Fig. 3(b), the asymmetry of EPR spectra of PC R_2 depends on the PANI doping level. Indeed, at $0\leqslant y\leqslant0.03$ the intensity of spectral positive peak is higher than that of negative peak of this PC spectrum. An opposite line asymmetry is demonstrated in PANI-ES samples with higher y [Fig. 3(b)]. The analysis of EPR spectra obtained at both waveband EPR's showed that the line asymmetry of R_2 PC in undoped and slightly doped PANI samples can be attributed to an anisotropy of the g factor which becomes more evident at the D band. At $y\geqslant0.21$ the line asymmetry is due to the appearance in the spectra of a Dyson-like component.[33] Such a Dyson-like line shape is commonly observed in 3-cm waveband EPR spectra of some inorganic substances,[34] organic conducting ion-radical salts,[35] *trans*-PA,[36] polythiophene,[37] poly(*para*-phenylene),[38] PANI,[39,40] and other conducting polymers.[20,27] The appearance of such a term in the EPR spectrum is caused by a skin-layer formation on a surface of a conducting sample due to the interaction of charge carriers with an electromagnetic polarizing field. The depth of the electromagnetic field penetration into a sample is limited by the skin-layer thickness δ, and depends on the sample paramagnetic susceptibility, which varies in a resonance region. This phenomenon affects the absorption of electromagnetic energy, incident on a sample. When the skin-layer thickness δ is less than that of a sample d, the time of charge-carrier diffusion through the skin layer becomes essentially less than a spin relaxation time. Therefore, when the size of a sample is comparable with the skin-layer thickness, a line becomes asymmetrical with an asymmetry factor A/B and shifts into lower fields.

In order to obtain all magnetic parameters of PC's in high-conductive PANI more correctly, the Dyson-like contribution to the total signal should be analyzed. In general, the sum spectra can be calculated from the equation for a first derivative of spectral contributions of dispersion $\chi^{|}$ and absorption $\chi^{\|}$ terms,[41]

$$\frac{d\chi}{dB}=Dg(\omega_e)+Ag^{|}(\omega_e), \tag{2}$$

where $g(\omega_e)$ is the line shape function,

$$D=\frac{1}{p^2+q^2}\times\frac{q\sinh p-p\sin q}{\cosh p+\cos q}+\frac{\sinh p\cdot\sin q}{(\cosh p+\cos q)^2}$$

and

$$A=\frac{1}{p^2+q^2}\times\frac{p\sinh p+q\sin q}{\cosh p+\cos q}+\frac{\cosh p\cdot\cos q+1}{(\cosh p+\cos q)^2}$$

are respectively the amplitudes of the dispersion and absorption signals: $p=2d/\delta\sqrt{\sqrt{1+\alpha^2}-\alpha}$, $q=2d/\delta\sqrt{\sqrt{1+\alpha^2}+\alpha}$, $\alpha=(\varepsilon\omega_e/4\pi\sigma_{ac})$, and $\delta=(\mu_0\omega_e\sigma_{ac}/2)^{-1/2}$.

Therefore, two type of PC's exist in PANI. The paramagnetic center R_1 with strongly asymmetric EPR spectrum can be attributed to a -(Ph-$NH^{\bullet+}$-Ph)t- radical with $g_{xx}=2.00603_2$, $g_{yy}=2.00381_5$, $g_{zz}=2.00239_0$, $A_{xx}=A_{yy}=4.5$ G, and $A_{zz}=30.2$ G, localized on a short polymer chain. The magnetic parameters of this radical differ weakly from those of the Ph-$NH^{\bullet}$-Ph radical,[42] probably because of a smaller delocalization of an unpaired electron on the nitrogen atom ($\rho_N^{pi}=0.39$) and of the more planar conformation of the latter. Assuming a McConnell proportionality constant

for the hyperfine interaction of the spin with nitrogen nucleus $Q=23.7$ G,[42] a spin density on the heteroatom nucleus of $\rho_N^{pi}(0)=(A_{xx}+A_{yy}+A_{zz})/(3Q)=0.55$ is estimated. At the same time another radical R_2 is formed in the system with $g_\perp=2.00439_4$ and $g_\parallel=2.00376_3$ which can be attributed to PC R_1 delocalized on more polymer units of a longer chain. The calculated spectra of these PC's are shown by dotted lines at the right of Fig. 3(b).

The lowest excited states ΔE_{ij} of the spin R_1 can be evaluated from their relation with respective g-factor shifts,[42] $\Delta E_{ij}=g_e\lambda_N\rho_N^\pi/(g_{xx,yy}-g_e)$, where g_e is the g factor of the free electron, λ_N is the constant of the spin-orbit interaction of an electron with a nitrogen nucleus, and ρ_N^π is the spin density on the π orbit of the nitrogen nucleus. For R_1 radical these energies were evaluated to be $\Delta E_{n\pi*}=2.9$ eV and $\Delta E_{\sigma\pi*}=7.1$ eV.

It was shown earlier[43] that g_{xx} and A_{zz} values of nitroxide radicals localized in a polymer are sensitive to changes in the radical microenvironmental properties, for example polarity and dynamics. The shift of the PC R_2 spectral X component to higher fields with y and/or a temperature increase may be interpreted not only by the growth of the polarity of the radical microenvironment, but also by the acceleration of the radical dynamics near its main molecular X axis. The effective g factors of both PC's are near to one another, i.e.,

$$\langle g\rangle_{R1}=(1/3)(g_{xx}+g_{yy}+g_{zz})\approx\langle g\rangle_{R2}=(1/3)(g_\parallel+2g_\perp).$$

This indicates that the mobility of a fraction of radicals R_1 along the polymer chain increases with polymer doping. Such a depinning of the mobility results in an exchange between the spectral components of the PC and, hence, to a decrease in the anisotropy of its EPR spectrum. In other words, radical R_1 transforms into radical R_2, which can be considered as a polaron diffusing along a polymer chain with a minimum rate[44] $\nu_{1D}^0\geqslant(g_{xx}-g_e)\mu_B h^{-1}B_0$, where B_0 is the resonance magnetic field, and $h=2\pi\hbar$ is the Planck constant. Using the g factors measured, we obtain $\nu_{1D}^0\geqslant 1.1\times10^8$ s^{-1}.

The g factor of PC R_2 in PANI with $y\geqslant0.21$ becomes isotropic and decreases from $g_{R2}=2.00418$ down to $g_{iso}=2.00314$. This is accompanied by a narrowing of the R_2 line (Fig. 3). Such effects can be explained by a further depinning of one-dimensional spin diffusion along the polymer chain, and therefore spin delocalization, and by the formation of areas with high spin density in which a strong spin-spin exchange on neighboring chains occurs. This is in agreement with the supposition[10,13] of formation in amorphous PANI-EB of high-conductive massive domains with 3D delocalized electrons.

The temperature dependences of ΔB_{pp} shown in Fig. 5 show evidence of different charge transport mechanisms in PANI with different conductivities. However, one can conclude that the mechanisms affecting the linewidth depend on the registration field: thus the linewidth does not directly reflects the relaxation and dynamics parameters of PC.

The doping of the PANI under study leads to an inverted Λ-like temperature dependence of an effective paramagnetic susceptibility (see Fig. 6), as occurs in the case of polyaniline perchlorate.[40] However, this does not lead to a strong narrowing of the PC line (Fig. 5). As in the case of PANI treated with ammonia, this should indicate a strong antiferromagnetic spin interaction due to a singlet-triplet equilibrium in the system under study; thus the total paramagnetic susceptibility can be written as[40]

$$\chi(T)=\mu_B^2 n(\varepsilon_F)+\frac{N_C g^2\mu_B^2}{4k_B(T+\theta)}+\frac{N_{TA}g^2\mu_B^2}{k_BT}\frac{\exp(-J/k_BT)}{1+3\exp(-J/k_BT)},\qquad(3)$$

where N_C and N_{TA} are the concentrations of the Curie and the thermally activated spins, respectively, and J is the interacting energy between spins.

As shown in Fig. 6, the paramagnetic susceptibility experimentally determined for the PANI samples is well reproduced by Eq. (3) with the parameters presented in Table I. The data of Table I show the prevalence of the Curie-like contribution in paramagnetic susceptibility for radicals in PANI with $y<0.21$, and this contribution decreases during polymer doping. The J value is close to that (0.078 eV) obtained for the ammonia treated PANI.[40]

Note that $n(\varepsilon_F)\approx1.3$–$2.8$ states/eV for two rings determined for PANI-H_2SO_4, consistent with those determined earlier for PANI heavily doped with other counterions.[45] With the assumption of a metallic behavior, from the data of Table I one can estimate that the energy of N_P Pauli spins in PANI, with $0.21\leqslant y\leqslant0.53$, $\varepsilon_F=3N_p/2n(\varepsilon_F)$ (Ref. 46), is to be 0.1–0.51 eV. This value is near to that (0.4 eV) obtained, e.g., for PANI doped with camphor sulfonic acid.[47] From this value the number of charge carriers with mass $m_c=m_e$ in heavily doped PANI,[46] $N_c=(2m_c\varepsilon_F/\hbar^2)^{3/2}/3\pi^2\approx1.7\times10^{21}$ cm^{-3}, is evaluated. The N_c value is close to a total spin concentration in PANI-H_2SO_4. This fact leads to the conclusion that all PC's take part in the polymer conductivity. For heavily doped PANI samples, the concentration of spin charge carriers is less than that of spinless ones, due to the possible collapse of pairs of polarons into diamagnetic bipolarons. Using lattice constant $c=0.96$ nm for PANI-H_2SO_4 (Ref. 14) the velocity of the charge carrier near the Fermi level can be calculated,[46] as $v_F=2c/[\pi\hbar n(\varepsilon_F)]=(3.3-7.2)\times10^7$ cm/s, typical for other conducting polymers.[26]

C. Spin relaxation and dynamics

Earlier, it was shown[43] that spin relaxation and dynamics in condensed systems, especially in conducting polymers,[26] can be analyzed from their 2-mm waveband EPR dispersion spectra. At this waveband an appreciable weakening of the exchange interaction between individual spin packets occurs at lower microwave power due to the increase in both the registration frequency and external magnetic field. Indeed, as for other organic conducting polymers,[26] both the 2-mm waveband EPR dispersion components of an initial and slightly doped PANI contain bell-like term with Gaussian

spin packet distributions (Fig. 4). Such an effect is as a result of the rapid passage of PC's when the conditions of the spin packet saturation $\gamma_e B_1 \sqrt{T_1 T_2} > 1$ and the adiabatic passage of resonance $dB/dt = B_m \omega_m < \gamma_e B_1^2$ hold, where γ_e is the gyromagnetic ratio of electron, B_1 is the magnetic component of the polarizing microwave field, T_1 and T_2 are the spin-lattice and spin-spin relaxation times, respectively, dB/dt is the rate of passage of the resonance, and B_m and ω_m are the amplitude and angular frequency of magnetic field modulation, respectively.

Generally, the first derivative of the dispersion signal consists of two in-phase and one $\pi/2$-out-of-phase terms[48]:

$$U = u_1 g'(\omega_m)\sin(\omega_m t) + u_2 g(\omega_m)\sin(\omega_m t - \pi) + u_3 g(\omega_m)\sin\left(\omega_m t \pm \frac{\pi}{2}\right). \quad (4)$$

Obviously, $u_2 = u_3 = 0$ in the absence of microwave saturation, and one registers an ordinary dispersion signal. In the opposite case all terms contribute EPR signal and the u_1 and u_3 intensities are determined by the ratio of the effective relaxation rate of spin packets $\tau^{-1} = (T_1 T_2)^{-1/2}$ and the rate of passage of resonance $\omega_m B_m$. If the latter is high and the modulation frequency is comparable with or higher than τ^{-1}, the spin packets have no time to track the reverse of the direction of the passage of the magnetic field because it proceeds at too high a rate. In the case of adiabatic passage of resonance each spin can see only an averaged applied magnetic field; therefore, the first derivative of the dispersion signal will be mainly determined by two last terms of Eq. (4), where $u_2 = \chi_0 \pi \gamma_e^2 B_1 B_m T_2/2$ and $u_3 = \chi_0 \pi \gamma_e^2 B_1 B_m T_2/(4\omega_m T_1)$. If the effective spin relaxation time is shorter than the modulation periods ($\tau < \omega_m^{-1}$) and $\tau > B_1/(dB/dt)$, the magnetization vector has sufficient time to recover to the equilibrium state during one modulation period. In this case the dispersion signal should be independent of the recording frequency, and will be mainly determined by the $u_1 g'(\omega_e)$ and $u_3 g(\omega_e)$ terms of Eq. (4), where $u_1 = \chi_0 \pi \gamma_e^2 B_1 B_m$ and $u_3 = \chi_0 \pi \gamma_e^2 B_1 B_m T_1 T_2/2$.

Thus the electronic relaxation times of the spin system can be determined from the components of the dispersion signal of saturated spin packets, recorded at corresponding phase tunings of the synchronous detector using the equations[28]

$$T_1 = \frac{3\omega_m(1+6\Omega)}{\gamma_e^2 B_{1_0}^2 \Omega(1+\Omega)}, \quad (5)$$

$$T_2 = \frac{\Omega}{\omega_m}, \quad (6)$$

(here $\Omega = u_3/u_2$ and B_{1_0} is the strength of the polarizing field at $u_1 = -u_2$) at $\omega_m T_1 > 1$,

$$T_1 = \frac{\pi u_3}{2\omega_m u_1}, \quad (7)$$

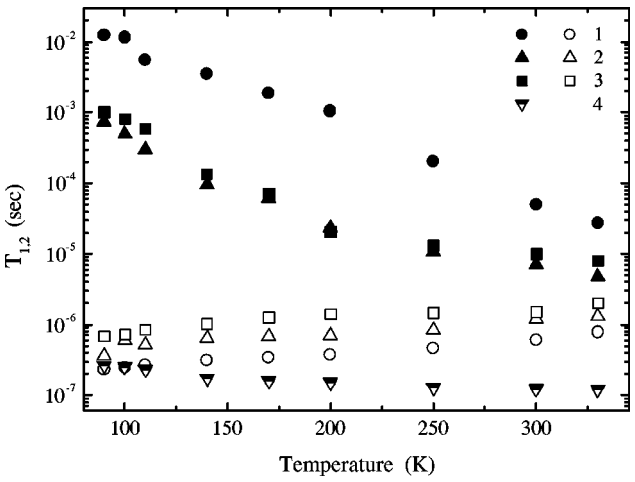

FIG. 8. Temperature dependence of the spin-lattice T_1 (filled points) and spin-spin T_2 (open points) relaxation times calculated from Eqs. (5), (6), (7), and (8) for PANI samples with doping levels of $y = 0.00$ (1), 0.01 (2), 0.03 (3), and 0.21 (4).

$$T_2 = \frac{\pi u_3}{2\omega_m(u_1 + 11u_2)} \quad (8)$$

at $\omega_m T_1 < 1$. The amplitudes of the u_i components are measured at the center of the spectrum, when $\omega = \omega_e$.

Relaxation times of an initial and slightly doped PANI-H_2SO_4 samples calculated from Eqs. (5), (6), (7), and (8) are shown in Fig. 8 as functions of temperature. Figure 8 demonstrates that the increase in the doping level of the polymer leads to shortening of the effective relaxation times of PC's, which can be due to an intensification of the spin exchange with the lattice and with other spins stabilized on neighboring polymer chains of highly conducting domains. It should be noted that spin relaxation in the polymer at high temperatures are mainly determined by the Raman interaction of the charge carries with lattice optical phonons. The probability and rate of such a process are dependent on the concentration n of the PC localized, e.g., in ionic crystals ($W_R \propto T_1^{-1} \propto n^2 T^7$) and in π-conjugated polymers ($W_R \propto T_1^{-1} \propto nT^2$).[49] The available data suggest that the T_1^{-1} values of PC's in polyaniline (with $y \leqslant 0.03$) are described by a dependence of the type $T_1^{-1} \propto nT^{-k}$, where $k = 3$–4, whereas those of PC's in the polymer with $y = 0.21$ are described by a flattened dependence characterized by the opposite sign of temperature variations, $T_1^{-1} \propto nT^{0.3}$ (see Fig. 8). This indicates the appearance of an additional channel of the energy transfer from the spin ensemble to the lattice at the polymer doping, as is the case in classical metals.

The relaxation times of electron and proton spins in PANI should vary depending on the spin precession frequency as $T_{1,2} \propto n^{-1} \nu_e^{1/2}$.[21] Therefore, the experimental data obtained can be explained by a modulation of electronic relaxation by 1D diffusion of R_2 radicals along the polymer chain, and by 3D hopping of these centers between chains with the diffusion coefficients D_{1D} and D_{3D}, respectively. In this case, the spectral density function for the spin mobility in the 1D system can be written as[50]

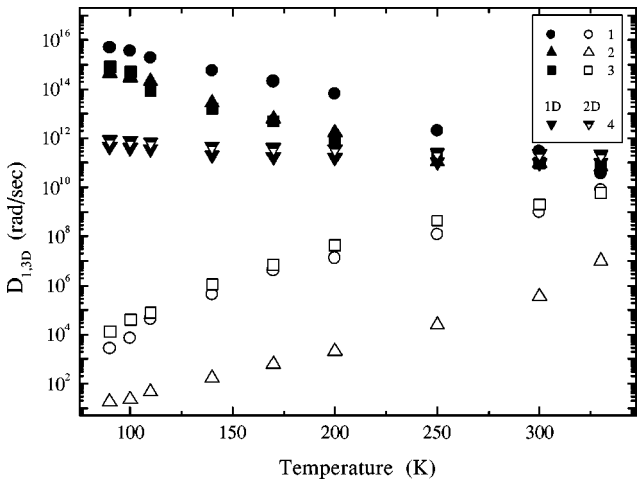

FIG. 9. Temperature dependence of the intrachain diffusion D_{1D} (filled points) and interchain hopping D_{3D} (open points) rates for polarons in the initial and H_2SO_4-doped PANI samples with $y=0.00$ (1), 0.01 (2), and 0.03 (3), as well as an effective rate of spin diffusion in PANI sample with $y=0.21$ calculated in the framework of 1D (filled points) and 2D (semifilled points) spin transport (4) respectively.

$$J(\omega_e)=n\phi_{1D}(\omega_e)\sum_{ij}, \tag{9}$$

where $n=n_1+n_2/\sqrt{2}$ is the effective concentration of both localized and delocalized PC's per the monomer unit of PANI, n_1 and n_2 are the relative concentrations of localized and delocalized PC's, respectively, Σ_{ij} is the lattice sum for the powderlike sample, $\phi_{1D}(\omega_e)=(2D^{|}_{1D}\omega_e)^{-1/2}$ at $D^{|}_{1D}\gg\omega_e\gg D_{3D}$ or $\phi_{1D}(\omega_e)=(2D^{|}_{1D}D_{3D})^{-1/2}$ at $D_{3D}\gg\omega_e$, $D^{|}_{1D}=4D_{1D}/N^2$, and N is the spin delocalization length in the monomer units. Previously,[21] an analogous spectral density function was used in the study of the spin dynamics in PANI. Note, however, that for 2D spin motion, $\phi_{2D}(\omega_e)=\ln(4\pi^2D_2/\omega_e)/2\pi\sqrt{D_1D_2}$.[51]

Since the electronic relaxation is mainly determined by the dipole-dipole interaction between localized and delocalized spins (with a spin value $S=1/2$), we can write the following equations for the rates of electronic relaxation[52]:

$$T_1^{-1}(\omega_e)=\langle\omega^2\rangle[2J(\omega_e)+8J(2\omega_e)], \tag{10}$$

$$T_2^{-1}(\omega_e)=\langle\omega^2\rangle[3J(0)+5J(\omega_e)+2J(2\omega_e)], \tag{11}$$

where $\langle\omega^2\rangle=0.1(\mu_0/4\pi)^2\gamma_e^4\hbar^2S(S+1)n\Sigma_{ij}$ is the averaged constant of the spin dipole interaction for a powderlike sample.

In Fig. 9 we show the temperature dependences of the effective dynamic parameters D_{1D} and D_{3D} calculated for both types of PC's in several PANI samples from the data presented in Fig. 8 using Eqs. (9)–(11) at $N\approx5$.[53] It seems to be justified that the anisotropy of the spin dynamics is maximum in the initial PANI sample, and decreases as y increases. At a relatively high degree of oxidation $y\geqslant0.21$, the electronic relaxation times become comparable and only slightly temperature dependent because of an intense spin-spin exchange in metal-like domains of higher effective dimensionalities. Providing that $T_1\cong T_2$ for the PANI sample with $y=0.21$, an effective rate of 1D and 2D spin motions in this polymer can be evaluated as well. It seems that both the rates calculated in the frameworks of 1D and 2D spin diffusions are near to one another.

It was found, at that 5–450-MHz waveband EPR (Ref. 21), that the high anisotropy of the spin dynamics is retained in PANI-HCl with $y=0.6$ even at room temperature. However, our experimental data indicate that the anisotropy of the motion of the charge carriers is high only in PANI-H_2SO_4 with $y<0.21$. Such a discrepancy is likely due to the fact that the effective dimensionality of PANI doped with H_2SO_4 to $y\geqslant0.21$ is larger than that of PANI-HCl. At $y\geqslant0.21$ the system seems to grow dimensionality in PANI-H_2SO_4, and at high temperatures the spin motion tends to become almost isotropic. The increase in the dimensionality at the polymer doping is accompanied by a decrease in the number of electron traps, which reduces the probability of electron scattering by the lattice phonons and results in the virtually isotropic spin motion and relatively slight temperature dependences of both the electronic relaxation and diffusion rates of PC's, as is the case for amorphous inorganic semiconductors.[29,46] This was also shown in a study of PANI-HCl with different doping levels at a 2-mm waveband.[18]

D. Charge transfer in undoped and H_2SO_4-doped polyaniline

To determine the conductivity components of a sample due to the mobility of the spin charge carriers, one can use well-known expression

$$\sigma_{1,3D}=n_2e^2D_{1,3D}c^2_{1,3D}/k_BT, \tag{12}$$

with $c_{1D}=0.960$ nm and $c_{3D}=0.590$ nm lattice constants of PANI-H_2SO_4.[14] In Fig. 10 the temperature dependences of conductivities due to 1D and 3D spin motions in PANI with $0.00\leqslant y\leqslant0.21$ are presented. In contrast with *trans*-PA, where an anisotropy of conductivity due to soliton dynamics, $A=\sigma_{1D}/\sigma_{3D}\approx10^5$ (at room temperature) does not change considerably upon the introduction of different dopants.[20,54] This parameter of PANI-H_2SO_4 decreases from 5×10^5 down to a unit as the doping level increases from 0.00 up to 0.21 (Fig. 10). An analogous decrease in the A value is also realized for PANI-HCl (Ref. 18) and other conducting polymers.[26] Note that this value was also determined by both EPR and NMR methods for heavily doped PANI-HCl to be near 20.[21] At the increase of the doping level from 0.01 up to 0.21 the σ_{ac}/σ_{dc} ratio changes from 6×10^3 to a unit (see Figs. 2 and 10). The same tendency was obtained in a study of microwave charge transport in PANI-ES (Ref. 55) and its derivatives.[13] This is additional evidence of a decrease in the anisotropy of the spin motion in PANI-ES, and is in agreement with the conclusions drawn previously concerning the growth of system dimensionality during the doping.[23] Another charge-transfer anisotropy can exist in the system. For instance, the ratio of dc conductivities measured along and across the stretch-oriented polymer chains, $\sigma_{\|}/\sigma_{\perp}$ depends

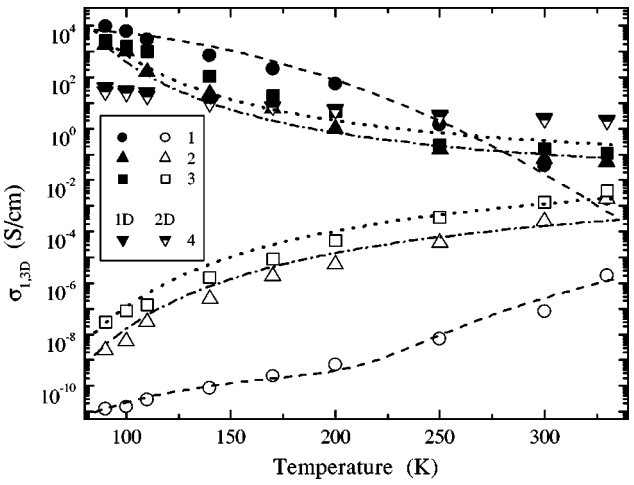

FIG. 10. Temperature dependence of the ac conductivity due to polaron motions along (filled points) and between (open points) polymer chains in the initial (1) and H_2SO_4-doped PANI samples with $y=0.01$ (2) and 0.03 (3) as well as an effective rate of spin diffusion in a PANI sample with $y=0.21$ (4), calculated, respectively, in the framework of 1D (filled points) and 2D (semifilled points) spin transport. The lines show the dependence calculated from Eq. (13) with $\sigma_0=2.7\times10^{-10}$ S K^{-1} s cm^{-1}, $k_3=3.1\times10^{12}$ s K$^{-9.5}$, and $m=8.5$ (above the dashed line), those calculated from Eq. (14) with the parameters $\sigma_0=3.95\times10^{-6}$ S cm^{-1} K^{-1} and $h\omega_{ph}=0.12$ eV (upper dash-dotted line), $\sigma_0=1.75\times10^{-6}$ S cm^{-1} K^{-1} and $h\omega_{ph}=0.11$ eV (upper dotted line); and those calculated from Eq. (15) with $\sigma^0_{3D}=8.2\times10^{-21}$ S K^{-1} s$^{0.8}$ cm^{-1} and $E_a=0.033$ eV (low-temperature region), $\sigma^0_{3D}=3.9\times10^{-12}$ S K^{-1} s$^{0.8}$ cm^{-1} and $E_a=0.41$ eV (high-temperature region) (lower dashed line), $\sigma^0_{3D}=4.5\times10^{-14}$ S K^{-1} s$^{0.8}$ cm^{-1} and $E_a=0.102$ eV (lower dash-dotted line), and $\sigma^0_{3D}=3.1\times10^{-13}$ S K^{-1} s$^{0.8}$ cm^{-1} and $E_a=0.103$ eV (lower dotted line).

upon the dopant types $10-10^4$ S/cm for PANI-ES (Refs. 10 and 56) and $20-10^3$ S/cm for *trans*-PA.[57]

The mechanism of spin and charge transport in PANI depends on the polymer doping level; therefore, the data obtained in the study of spin dynamics in PANI-H_2SO_4 can be interpreted using different models for the charge transfer in low-dimensional systems. Previously,[18] we interpreted the dynamic process occurring in PANI-HCl as the motion of a small polaron in an undoped sample and interchain spin hopping in a slightly doped ($y=0.03$) polymer in the framework of Kivelson theory.[9]

The fact that the spin-lattice-relaxation time of PANI is strongly dependent on the temperature (see Fig. 8) means that, in accord with the energy conservation law, electron hops should be accompanied by the absorption or emission of a minimum number of lattice phonons. Multiphonon processes become predominant in neutral PANI because of a strong spin-lattice interaction. For this reason, an electronic dynamics process occurring in the polymer should be considered in the framework of Kivelson's formalism[9] of isoenergetic electron transfer between the polymer chains involving optical phonons, because spin and spinless charge carriers probably exist even in an undoped polymer (see Fig. 3). According to this model, the Coulomb interaction occurs between the charge carriers and the dopant anions introduced into the polymer. In this case, the excess charge can be isoenergetically transferred from one charge carrier to another charge carrier moving along the neighboring polymer chain. The temperature dependence of the probability of this process and, hence, of the charge-carrier mobility, will be determined by the probability of finding the neutral soliton or polaron near the dopant anion. The ac conductivity is defined by the expression[9,58]

$$\sigma_{ac}(T)=\frac{N_i^2e^2\langle y\rangle\xi_\parallel^3\xi_\perp^2\nu_e}{384k_BT}\left[\ln\frac{2\nu_eL}{\langle n\rangle\gamma(T)}\right]^4=\frac{\sigma_0\nu_e}{T}\left[\ln\frac{k_3\nu_e}{T^{m+1}}\right]^4, \tag{13}$$

where $k_1=0.45$, $k_2=1.39$, and k_3 are constants; $\gamma(T)=\gamma_0(T/300\ \mathrm{K})^{m+1}$ is the rate of electron transfer between the charge carriers; $\langle n\rangle=n_pn_{bp}(n_p+n_{bp})^{-2}$, where n_p and n_{bp} are the concentrations of polarons and bipolarons per the monomer unit of the polymer chain, respectively, $R_0=(4\pi N_i/3)^{-1/3}$ is the typical distance between the dopant anions with the concentration N_i; $\xi=(\xi_\parallel\xi_\perp^2)^{1/3}$, $\xi_\parallel$, and $\xi_\perp$ are the averaged localization length of the wave function of the charge carrier and its parallel and perpendicular components, respectively; L is the number of monomer units in the polymer chain; and $m\approx10$.

Figure 10 shows that the experimental data for σ_{1D} of the initial PANI sample is fitted well by Eq. (13) with $\sigma_0=2.7\times10^{-10}$ S K s cm^{-1}, $k_3=3.1\times10^{12}$ s K$^{9.5}$, and $m=8.5$. In contrast to undoped *trans*-PA, some quantity of charged carriers exist even in the initial PANI sample, so the above Kivelson mechanism can determine its conductivity. Such an approach is not evident for PANI with $0.01\leqslant y\leqslant0.03$ due to lower temperature dependence of these samples. The model of charge-carrier scattering by optical phonons of the lattice of metal-like domains in conjugated polymers[16,59] seems to be more convenient for the explanation of the behavior of their conductivity. In the framework of this model the conductivity of a slightly doped polymer can be expressed as

$$\sigma_{ac}(T)=\frac{Ne^2\omega_{ph}c_{1D}Mt_0^2k_BT}{4\hbar^3\alpha^2}[\sinh(h\omega_{ph}/k_BT)-1]$$

$$=\sigma_0T[(h\omega_{ph}/k_BT)-1], \tag{14}$$

where M is the mass of the CH or NH group, t_0 is a transfer integral equal to 2–3 eV for the π electron, ω_{ph} is the frequency of the optical phonon, and α is the constant of electron-phonon interaction [for *trans*-PA α is equal to 4.1×10^8 eV cm^{-1} (Ref. 16)].

As can be seen in Fig. 10, the $\sigma_{1D}(T)$ dependence for the PANI-H_2SO_4 sample with $y=0.01$ and 0.03 is fairly well fitted using Eq. (14) with $h\omega_{ph}=0.12$ and 0.11 eV, respectively. The latter values are near to an energy (0.19 eV) of the polaron pinning in heavily doped PANI-ES.[55]

The strong temperature dependence σ_{3D} of the initial sample can probably be interpreted in the framework of the model for the activation (with the activation energy E_a) charge transfer between the polymer chains,[29]

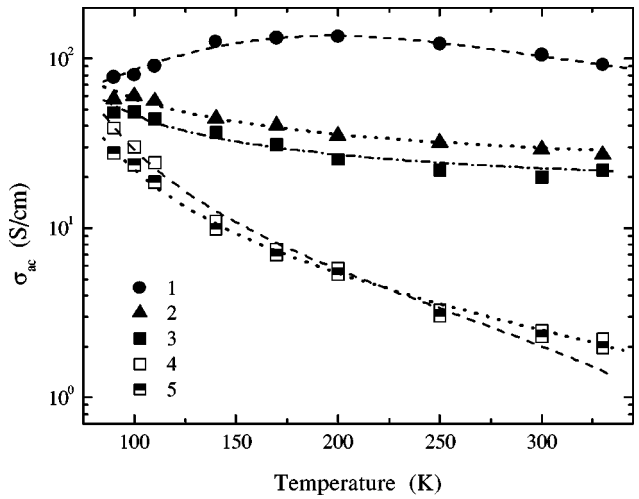

FIG. 11. Temperature dependence of the ac conductivity calculated from the Dyson-like EPR line of H_2SO_4-doped PANI samples with $y=0.53$ (1), 0.42 (2), and 0.21 (3), and these determined from spin relaxation of PC in PANI with $y=0.21$ in the framework of 1D (4) and 2D (5) spin motions. The lines show the dependences calculated from Eq. (17) with $\sigma_{0_1}=0.86$ S cm^{-1} K^{-1}, $\sigma_{0_2}=2.1\times10^{-2}$ S cm^{-1} K^{-1}, and $h\omega_{ph}=0.087$ eV (upper dashed line); and those calculated from Eq. (14) with $\sigma_0=1.5\times10^{-1}$ S cm^{-1} K^{-1} and $h\omega_{ph}=0.013$ eV (middle dotted line), $\sigma_0=5.8\times10^{-2}$ S cm^{-1} K^{-1} and $h\omega_{ph}=0.017$ eV (middle dash-dotted line), $\sigma_0=1.47\times10^{-2}$ S cm^{-1} K^{-1} and $h\omega_{ph}=0.027$ eV (lower dashed line), and $\sigma_0=1.49\times10^{-2}$ S cm^{-1} K^{-1} and $h\omega_{ph}=0.025$ eV (lower dotted line).

$$\sigma_{3D}(T)=\sigma_{3D}^0\nu_e^{0.8}T\exp(-E_a/k_BT), \tag{15}$$

with E_a equal to 0.033 and 0.41 eV for low- and high-temperature regions, respectively (Fig. 10). The activation energy of interchain charge transfer in slightly doped samples is $E_a=0.102$ eV for PANI with $y=0.01$ and $E_a=0.103$ eV for PANI with $y=0.03$ (Fig. 10).

Note that the spin diffusion coefficients and consequently the conductivities, calculated from the spin relaxation of PANI with $y=0.21$, in frameworks of one- and two-dimensional spin diffusion, are near to one another (Figs. 9 and 10). This fact can possibly be interpreted as the result of the increase of system dimensionality above the percolation border (around $y\approx0.1$). However, this can be also due to the decrease in accuracy of the saturation method at high doping levels. In this case the dynamics parameters of both spin and spinless charge carriers can be evaluated from the Dyson-like EPR spectrum.

Figure 11 shows the temperature dependence of the ac conductivity of doped PANI samples determined from their Dysonian 2-mm EPR spectra using Eq. (2). For the comparison, the conductivities determined for PANI with $y=0.21$ in the framework of 1D and 2D spin motions (Fig. 10) are presented as well. The charge transport properties determined for the latter sample by different methods seems to differ. In contrast with the shape of the saturated dispersion EPR signal, the Dyson-like line shape ''feels'' both types of charge carriers, spin polarons, and spinless bipolarons, as effective charge ensemble, diffusing through a skin layer. The number and dynamics of this type of charge carriers can differ; thus the electronic dynamics properties of the sample should depend on its doping level. Indeed, the conductivity determined from the Dyson-like absorption spectra of PANI with $y=0.21$ is higher than that calculated from its dispersion ones (Fig. 11). The slopes of their temperature dependences are different as well. This fact provides additional evidence of the appearance in doped PANI samples of diamagnetic bipolarons or other types of charge carriers, i.e., 3D delocalized conducting electrons are the main charge carriers in doped samples. Using the data presented in Fig. 11 and in Table I, from Eq. (12) we can evaluate the ratio of the diffusing coefficients of these charge carriers, equal approximately to 0.39 at room temperature.

The slope of the temperature dependences of conductivity of PANI with $y=0.21$ and 0.42, shown in Fig. 11, can also be explained by the interaction of charge carriers with the lattice phonons described by Eq. (14). Figure 11 shows that the experimental σ_{ac} values obtained for PANI with $y=0.21$ in frames with spins of 1D and 2D diffusion are fitted well by Eq. (14) with $h\omega_{ph}=0.027$ eV and $h\omega_{ph}=0.025$ eV, respectively. Assuming that both types of charge carriers take part in the conductivity of this sample, for this case one obtains $h\omega_{ph}=0.017$ eV or $\nu_{ph}=4.17\times10^{12}$ s^{-1} (see Fig. 11). Equation (14) also fits the conductivity data of PANI with $y=0.42$ if $h\omega_{ph}=0.013$ eV (Fig. 11).

The conductivity calculated from Dysonian absorption spectra of the heavily doped PANI sample demonstrates an extremal temperature dependence with a characteristic point $T_c\cong200$ K. An analogous dependency was obtained earlier for PANI-HCl with $y=0.41$ and 0.50.[18] Such a temperature dependency can be attributed to the above-mentioned interacting charge carriers with lattice phonons at high temperatures the [metallic regime described by Eq. (14)] and by their Mott VRH at low temperatures (the semiconducting regime). The latter approach gives, for the ac conductivity,[29]

$$\sigma_{ac}(T)=(1/3)\pi e^2k_BTn^2(\varepsilon_F)\alpha^{-5}\omega_e\ln^4(\omega_0/\omega_e)=\sigma_0T, \tag{16}$$

where ω_0 is the angular limiting hopping frequency.

It is seen from Fig. 11 that the combination of Eqs. (14) and (16),

$$\sigma_{ac}(T)=\{\sigma_{0_1}^{-1}T^{-1}+\sigma_{0_2}^{-1}T^{-1}[\sinh(h\omega_{ph}/k_BT)-1]^{-1}\}^{-1}, \tag{17}$$

with $\sigma_{0_1}=0.86$ S cm^{-1}K^{-1}, $\sigma_{0_2}=2.1\times10^{-2}$ S cm^{-1}K^{-1}, and $h\omega_{ph}=0.087$ eV, well fits the conductivity of a heavily doped PANI-H_2SO_4 sample. The latter value is larger than $h\omega_{ph}=0.018$ eV determined for PANI-HCl (Ref. 18), but lies near to the value of $h\omega_0=0.066$ eV evaluated from the data obtained by Wang and co-workers.[10,13]

The ac conductivity of heavily doped PANI-H_2SO_4, estimated from the contribution of spin charge carriers, is about 110 S cm^{-1} at room temperature (see Fig. 11). This value is much smaller than $\sigma_{ac}(\omega_e\rightarrow\infty)\cong10^7$ S cm^{-1} calculated theoretically;[15] however, it lies near that obtained for metal-like domains in PANI at 6.5 GHz.[15] The σ_{ac}/σ_{dc} ratio for

these domains can now be evaluated for the PANI under study to be 4.5, that is near to that obtained for PANI doped by some mineral acids.[60] Taking into account that the $\sigma_{ac} \cong \sigma_{dc}$ condition is fulfilled for classic metals,[46] one can conclude a good structural ordering of these domains. Charge carriers diffuse along the polymer chains with the constant $D_{1D}=\sigma_{ac}e^{-2}n^{-1}(\varepsilon_F)c_{1D}^{-2}$, that is near to 8.3×10^{12} rad/s; in addition, their mean free path $l_i=\sigma_{ac}m_c v_F/(Ne^2)$ is near to 0.5 nm at room temperture. The latter value is smaller than that estimated for oriented *trans*-PA (Ref. 16) and PANI-HCl,[18] but also holds for extended electron states in PANI-H_2SO_4 as well. The energy of lattice phonons $h\omega_{ph}$ obtained from ac data correlates with the energy J of the interaction between spins (see Figs. 6, 10, and 11), that shows the modulation of spin-spin interaction by macromolecular dynamics in the system.

IV. CONCLUSION

The combination of EPR and electron transport studies shows that two types of paramagnetic centers are formed in PANI, polarons localized on chains in amorphous polymer regions and polarons moving along and between polymer chains. The number of the latter increases during the polymer doping. After the percolation border the interaction between spin charge carriers and their mobility increases, so part of the mobile polarons collapses into diamagnetic bipolarons. This process is modulated by macromolecular dynamics, and is accompanied by an increase in the crystalline order (or dimensionality) and planarity of the system.

During polymer doping the conducting single chains become crystallization centers for the formation in amorphous regions of the massive metal-like domains of strongly coupled chains with 3D delocalized charge carriers. The charge 3D and 1D hops between these domains in the medium and heavily doped PANI, respectively. The doping changes the interaction of the charge carriers with the lattice phonons, and therefore the mechanism of charge transfer. It also results in an increase of the number and size of highly conducting domains containing charge carriers of different types and mobilities, which lead to an increase in the conductivity and Pauli susceptibility above the percolation boundary.

In the initial PANI the charges are transferred isoenergetically between solitary chains in the framework of the Kivelson formalism. The growth of the system dimensionality leads to the scattering of charge carriers on the lattice phonons. In heavily doped PANI the charge carriers are transferred according to the variable range hopping mechanism, and are scattered on the lattice phonons as well. This is in agreement with the concept of the presence of 3D domains in PANI-ES (Refs. 10 and 13) rather than the supposition that 1D solitary conducting chains exist even in heavily doped PANI.

ACKNOWLEDGMENTS

We would like to thank Dr. S.D. Chemerisov and I. B. Nazarova for assistance with the EPR experiment, and Dr. A.S. Astakhova for performing the elemental analysis of the PANI powders. This work was supported in part by the Russian Foundation for Basic Researches, Grant No. 01-03-33255a.

[1] *Electronic Properties of Polymers*, edited by H. Kuzmany, M. Mehring, and S. Roth (Springer, Berlin, 1992); *Organics Conductors. Fundamentals and Applications*, edited by J. P. Ferges (Dekker, New York, 1994); *Handbook of Organic Conductive Molecules and Polymers*, **1-4**, edited by H. S. Nalwa (Wiley, Chichester, 1997); *Handbook of Conducting Polymers*, edited by T. E. Scotheim, R. L. Elsenbaumer, and J. R. Reynolds (Dekker, New York, 1997).

[2] A. A. Syed and M.K. Dinesan, Talanta **38**, 815 (1991); D. C. Trivedi, in *Handbook of Organic Conductive Molecules and Polymers*, edited by H. S. Nalwa (Wiley, Chichester, 1997), Vol. 2, p. 505.

[3] F. Wudl, R.O. Angus, F.L. Lu, P.M. Allemand, D.J. Vachon, M. Nowak, Z.X. Liu, and A.J. Heeger, J. Am. Chem. Soc. **109**, 3677 (1987).

[4] A.J. Epstein, J.M. Ginder, F. Zuo, R.W. Bigelow, H.S. Woo, D.B. Tanner, A.F. Richter, W.S. Huang, and A.G. MacDiarmid, Synth. Met. **18**, 303 (1987).

[5] Y. Cao, P. Smith, and A.J. Heeger, Synth. Met. **48**, 91 (1992); M. Reghu, Y. Cao, D. Moses, and A.J. Heeger, Phys. Rev. B **47**, 1758 (1993).

[6] Y. Onodera, Phys. Rev. B **30**, 775 (1984).

[7] J.L. Brédas, B. Themans, J.G. Fripiat, J.M. Andre, and R.R. Chance, Phys. Rev. B **29**, 6761 (1984).

[8] S. Stafström, J.L. Brédas, A.J. Epstein, H.S. Woo, D.B. Tanner, W.S. Huang, and A.G. MacDiarmid, Phys. Rev. Lett. **59**, 1464 (1987).

[9] S. Kivelson, Phys. Rev. Lett. **46**, 1344 (1981); Bull. Am. Phys. Soc. **26**, 383 (1981); Mol. Cryst. Liq. Cryst. **77**, 65 (1981); Phys. Rev. B **25**, 3798 (1982).

[10] Z.H. Wang, E.M. Scherr, A.G. MacDiarmid, and A.J. Epstein, Phys. Rev. B **45**, 4190 (1992); Z.H. Wang, C. Li, E.M. Scherr, A.G. MacDiarmid, and A.J. Epstein, Phys. Rev. Lett. **66**, 1745 (1991); K.R. Cromack, M.E. Jozefowicz, J.M. Ginder, A.J. Epstein, R.P. McCall, G. Du, J.M. Leng, K. Kim, C. Li, Z.H. Wang, M.A. Druy, P.J. Gltkowski, E.M. Scherr, and A.G. MacDiarmid, Macromolecules **24**, 4157 (1991).

[11] H.Y. Choi and E.J. Mele, Phys. Rev. Lett. **59**, 2188 (1987).

[12] B. Abeles, P. Sheng, M.D. Coutts, and Y. Arie, Adv. Phys. **24**, 407 (1975).

[13] Z.H. Wang, A.J. Epstein, A. Ray, and A.G. MacDiarmid, Synth. Met. **41**, 749 (1991); J.P. Pouget, S.L. Zhao, Z.H. Wang, Z. Oblakowski, A.J. Epstein, S.K. Manohar, J.M. Wiesingr, A.G. MacDiarmid, and C.H. Hsu, *ibid.* **55**, 341 (1993); Z.H. Wang, A. Ray, A.G. MacDiarmid, and A.J. Epstein, Phys. Rev. B **43**, 4373 (1991); Z.H. Wang, H.H.S. Javadi, A. Ray, A.G. MacDiarmid,

and A.J. Epstein, *ibid.* **42**, 5411 (1990).
[14] J.P. Pouget, M.E. Jozefowicz, A.J. Epstein, X. Tang, and A.G. MacDiarmid, Macromolecules **24**, 779 (1991); M.E. Jozefowicz, R. Laversanne, H.H.S. Javadi, A.J. Epstein, J.P. Pouget, X. Tang, and A.G. MacDiarmid, Phys. Rev. B **39**, 12 958 (1989).
[15] J. Joo, E.J. Oh, G. Min, A.G. MacDiarmid, and A.J. Epstein, Synth. Met. **69**, 251 (1995).
[16] S. Kivelson and A.J. Heeger, Synth. Met. **22**, 371 (1988).
[17] J.M. Ginder, A.F. Richter, A.G. MacDiarmid, and A.J. Epstein, Solid State Commun. **63**, 97 (1987).
[18] V.I. Krinichnyi, S.D. Chemerisov, and Y.S. Lebedev, Phys. Rev. B **55**, 16 233 (1997); Synth. Met. **84**, 819 (1997); Polym. Sci. A **40**, 826 (1998).
[19] K. Lee, A.J. Heeger, and Y. Cao, Synth. Met. **72**, 25 (1995); K. Lee and A.J. Heeger, *ibid.* **84**, 715 (1997).
[20] K. Mizoguchi and S. Kuroda, in *Handbook of Organic Conductive Molecules and Polymers*, edited by H. S. Nalwa (Wiley, Chichester, 1997), Vol. 3, p. 251.
[21] K. Mizoguchi, M. Nechtschein, J.-P. Travers, and C. Menardo, Phys. Rev. Lett. **63**, 66 (1989); K. Mizoguchi, M. Nechtschein, and J.-P. Travers, Synth. Met. **41**, 113 (1991); K. Mizoguchi and K. Kume, *ibid.* **69**, 241 (1995); M. C. Itow, T. Kawahara, N. Kachi, H. Sakamoto, K. Mizoguchi, K. Kume, Y. Sahara, S. Masubuchi, and S. Kazama, *ibid.* **84**, 749 (1997).
[22] D.S. Galvao, D.A. don Santos, B. Laks, C.P. de Melo, and M.J. Caldas, Phys. Rev. Lett. **63**, 786 (1989); L.W. Shacklette and R.H. Baughman, Mol. Cryst. Liq. Cryst. **189**, 193 (1990).
[23] F. Lux, G. Hinrichsen, V.I. Krinichnyi, I.B. Nazarova, S.D. Chemerisov, and M.M. Pohl, Synth. Met. **55**, 347 (1993); H.-K. Roth and V.I. Krinichnyi, Makromol. Chem., Macromol. Symp. **72**, 143 (1993).
[24] F. Lux, Ph.D. Thesis, Technical University, 1993, Berlin; F. Lux, Polymer **35**, 2915 (1994); F. Lux, G. Hinrichsen, and M.M. Pohl, J. Polym. Sci., Part B: Polym. Phys. **32**, 1957 (1994).
[25] A.A. Galkin, O.Y. Grinberg, A.A. Dubinskii, N.N. Kabdin, V.N. Krymov, V.I. Kurochkin, Y.S. Lebedev, L.G. Oransky, and V.F. Shuvalov, Instrum. Exp. Tech. **20**, 1229 (1977).
[26] V. I. Krinichnyi, *2-mm Wave Band EPR Spectroscopy of Condensed Systems* (CRC Press, Boca Raton, FL, 1995); V.I. Krinichnyi, Russ. Chem. Rev. **65**, 521 (1996); V.I. Krinichnyi, Synth. Met. **108**, 173 (2000).
[27] P. Bernier, in *Handbook of Conducting Polymers*, edited by T. E. Scotheim (Dekker, New York, 1986), Vol. 2, p. 1099.
[28] A.E. Pelekh, V.I. Krinichnyi, A.Y. Brezgunov, L.I. Tkachenko, and G.I. Kozub, Vysokomolekul.Soedin. A **33**, 1731 (1991).
[29] N. F. Mott and E. A. Davis, *Electronic Processes in Non-Crystalline Materials*, (Clarendon Press, Oxford, 1979).
[30] P. K. Kahol, N. J. Pinto, E. J. Berndtsson, and B. J. McCormick, J. Phys. **6**, 5631 (1994).
[31] D.K. Paul and S.S. Mitra, Phys. Rev. Lett. **31**, 1000 (1973); K. Nair and S.S. Mitra, Non-Cryst. Solids **24**, 1 (1977).
[32] N.J. Pinto, P.K. Kahol, B.J. McCormick, N.S. Dalal, and H. Wan, Phys. Rev. B **49**, 13 983 (1994).
[33] F.J. Dyson, Phys. Rev. B **98**, 349 (1955).
[34] Z. Wilamowski, B. Oczkiewicz, P. Kacman, and J. Blinowski, Phys. Status Solidi B **134**, 303 (1986).
[35] J. M. Williams, J. R. Ferraro, R. J. Thorn, K. D. Carlson, U. Geiser, H. H. Wang, A. M. Kini, and M.-H. Whangboo, *Organic Superconductors (Including Fullerenes): Synthesis, Structure, Properties, and Theory* (Prentice-Hall, Englewood Cliffs, NJ, 1992).
[36] I.B. Goldberg, H.R. Crowe, P.R. Newman, A.J. Heeger, and A.G. MacDiarmid, J. Chem. Phys. **70**, 1132 (1979); P. Bernier, Mol. Cryst. Liq. Cryst. **83**, 1089 (1982); R. Cosmo, E. Dormann, B. Gotschy, H. Naarmann, and H. Winter, Synth. Met. **41**, 369 (1991); D. Billand, F.X. Henry, and P. Willmann, *ibid.* **69**, 9 (1995).
[37] G. Tourillon, in *Handbook of Conducting Polymers*, edited by T. E. Scotheim, **1** (Dekker, New York, 1986), p. 293.
[38] L. M. Goldenberg, A.E. Pelekh, V.I. Krinichnyi, O.S. Roshchupkina, A.F. Zueva, R.N. Lyubovskaja, and O.N. Efimiv, Synth. Met. **36**, 217 (1990).
[39] A.P. Monkman, D. Bloor, and G.C. Stevens, J. Phys. D **23**, 627 (1990).
[40] M. Iida, T. Asaji, M.B. Inoue, and M. Inoue, Synth. Met. **55**, 607 (1993).
[41] I.G. Zamaleev, A.R. Kessel, and G. B. H. Teitelbaum, Fizika Met. Metalloved. **34**, 16 (1972) [Phys. Met. Metallogr. **34**, 15 (1972)]; T.S. Altshuler, O.B. Vinogradova, A.F. Kukovitski, and E.G. Harahashjan, Fiz. Tverd. Tela (Leningrad) **15**, 3602 (1973) [Sov. Phys. Solid State **15**, 3602 (1973)].
[42] A. L. Buchachenko and A. M. Vasserman, *Stable Radicals* (Khimija, Moscow, 1973) (in Russian).
[43] V.I. Krinichnyi, Appl. Magn. Reson. **2**, 29 (1991); J. Biochem. Biophys. Methods **23**, 1 (1991).
[44] Ch. P. Poole, *Electron Spine Resonance* (International Science Publishers, London, 1967).
[45] K. Lee, A.J. Heeger, and Y. Cao, Synth. Met. **69**, 261 (1995); J.M. Ginder, A.F. Richter, A.G. MacDiarmid, and A.J. Epstein, Solid State Commun. **63**, 97 (1987); P.K. Kahol, N.J. Pinto, and B.J. McCormick, *ibid.* **91**, 21 (1994).
[46] G. S. Blakemore, *Solid State Physics* (Cambridge University Press, Cambridge, 1985).
[47] K.H. Lee, A.J. Heeger, and Y. Cao, Phys. Rev. B **48**, 14 884 (1993).
[48] P.R. Gullis, J. Magn. Reson. **21**, 397 (1976).
[49] S.P. Kurzin, B.G. Tarasov, N.F. Fatkullin, and R.M. Aseeva, Vysokomolekul. Soedin. A **24**, 117 (1982).
[50] M.A. Butler, L.R. Walker, and Z. G. Soos, J. Chem. Phys. **64**, 3592 (1976).
[51] M. Nechtschein, in *Handbook of Conducting Polymers*, edited by T. A. Skotheim, R. L. Elsenbaumer, and J. R. Reynolds (Dekker, New York, 1997), p. 141.
[52] A. Abragam, *The Principles of Nuclear Magnetism* (Clarendon Press, Oxford, 1961); F. Carrington and A. D. McLachlan, *Introduction to Magnetic Resonance with Application to Chemistry and Chemical Physics* (Harrer & Row, New York, 1967); *Theoretical Foundation of Electron Spin Resonance*, edited by J. E. Hamman (Academic Press, New York, 1978); H.-K. Roth, F. Keller, and H. Schneider, *Hochfrequenzspectroskopie in der Polymerforschung* (Academie Verlag, Berlin, 1984).
[53] F. Devreux, F. Genoud, M. Nechtschein, and B. Villeret, in *Electronic Properties of Conjugated Polymers*, edited by H. Kuzmany, M. Mehring, and S. Roth, Springer Series in Solid State Sciences Vol. 76 (Springer-Verlag, Berlin, 1987), p. 270.
[54] M. Nechtschein, F. Devreux, R.L. Greene, T.C. Clarke, and G.B. Street, Phys. Rev. Lett. **44**, 356 (1980); M. Nechtschein and Y.W. Park, Synth. Met. **69**, 77 (1995).

[55] H.H.S. Javadi, K.R. Cromack, A.G. MacDiarmid, and A.J. Epstein, Phys. Rev. B **39**, 3579 (1989).
[56] M. Costolo and A.J. Heeger, Synth. Met. **114**, 85 (2000).
[57] H.A. Mizes and E.M. Conwell, Phys. Rev. B **43**, 9053 (1991); A.J. Heeger, S. Kivelson, J.R. Schrieffer, and W.P. Su, Rev. Mod. Phys. **60**, 781 (1988); S. Stafström, Phys. Rev. B **47**, 12 437 (1993); C.O. Yoon, Y.W. Park, K. Akagi, and H. Shirakawa, Mol. Cryst. Liq. Cryst. **224**, 69 (1993); Y.W. Park, C. Park, Y.S. Lee, C.O. Yoon, H. Shirakawa, Y. Suezaki, and K. Akagi, Solid State Commun. **65**, 147 (1988).
[58] P. Kuivalainen, H. Stubb, H. Isotalo, P. Ylilahti, and C. Holmström, Phys. Rev. B **31**, 7900 (1985).
[59] L. Pietronero, Synth. Met. **8**, 225 (1983).
[60] V.I. Krinichnyi, A.L. Konkin, P. Devasagayam, and A.P. Monkman, Synth. Met. **119**, 281 (2001).